

## Changing the three-dimensional magnetization exchange coupling of mixed Fe and V nanoclusters with hydrogen

V. K. Valev, M. Di Vece, M. J. Van Bael, D. Grandjean, S. Decoster et al.

Citation: *J. Appl. Phys.* **105**, 114907 (2009); doi: 10.1063/1.3133233

View online: <http://dx.doi.org/10.1063/1.3133233>

View Table of Contents: <http://jap.aip.org/resource/1/JAPIAU/v105/i11>

Published by the AIP Publishing LLC.

### Additional information on J. Appl. Phys.

Journal Homepage: <http://jap.aip.org/>

Journal Information: [http://jap.aip.org/about/about\\_the\\_journal](http://jap.aip.org/about/about_the_journal)

Top downloads: [http://jap.aip.org/features/most\\_downloaded](http://jap.aip.org/features/most_downloaded)

Information for Authors: <http://jap.aip.org/authors>

## ADVERTISEMENT

# Instruments for advanced science

### Gas Analysis



- dynamic measurement of reaction gas streams
- catalysis and thermal analysis
- molecular beam studies
- dissolved species probes
- fermentation, environmental and ecological studies

### Surface Science



- UHV TPD
- SIMS
- end point detection in ion beam etch
- elemental imaging - surface mapping

### Plasma Diagnostics



- plasma source characterization
- etch and deposition process
- reaction kinetic studies
- analysis of neutral and radical species

### Vacuum Analysis



- partial pressure measurement and control of process gases
- reactive sputter process control
- vacuum diagnostics
- vacuum coating process monitoring

contact Hiden Analytical for further details

**HIDEN**  
ANALYTICAL

[info@hideninc.com](mailto:info@hideninc.com)  
[www.HidenAnalytical.com](http://www.HidenAnalytical.com)

CLICK to view our product catalogue



# Changing the three-dimensional magnetization exchange coupling of mixed Fe and V nanoclusters with hydrogen

V. K. Valev,<sup>1</sup> M. Di Vece,<sup>2,a)</sup> M. J. Van Bael,<sup>2</sup> D. Grandjean,<sup>2</sup> S. Decoster,<sup>3</sup> A. Vantomme,<sup>3</sup> T. Verbiest,<sup>1</sup> and P. Lievens<sup>2</sup>

<sup>1</sup>*Molecular Electronics and Photonics, INPAC-Institute for Nanoscale Physics and Chemistry, Katholieke Universiteit Leuven, Celestijnenlaan 200 D, B-3001 Leuven, Belgium*

<sup>2</sup>*Laboratorium voor Vaste-Stoffysica en Magnetisme and INPAC-Institute for Nanoscale Physics and Chemistry, Katholieke Universiteit Leuven, Celestijnenlaan 200D, B-3001, Heverlee, Belgium*

<sup>3</sup>*Instituut voor Kern-en Stralingsfysica and INPAC-Institute for Nanoscale Physics and Chemistry, Katholieke Universiteit Leuven, Celestijnenlaan 200D B-3001 Leuven, Belgium*

(Received 7 January 2009; accepted 21 April 2009; published online 4 June 2009)

The magneto-optical Kerr effect of an iron-vanadium nanocluster-assembled thin film was measured as a function of hydrogen content. Hydrogen has a clear effect on the magnetization of this three-dimensional exchange coupled system for both increasing and decreasing hydrogen pressures. This effect is attributed to the modification of the electronic properties of the nonmagnetic vanadium nanoclusters by hydrogen. Since vanadium mediates the exchange coupling between aggregated iron nanoclusters, the changes in magnetic properties are directly related to hydrogen absorption.

© 2009 American Institute of Physics. [DOI: [10.1063/1.3133233](https://doi.org/10.1063/1.3133233)]

## I. INTRODUCTION

When the dimensions of matter are reduced to the nanoscale, new and exotic physical properties of materials are revealed. An example of nanoscale effects in the field of magnetism is interlayer exchange coupling in heterostructures by which the magnetic state depends on the interlayer distance.<sup>1</sup> It is one of the many noticeable discoveries of the last fifty years, which also include giant magnetoresistance,<sup>2-4</sup> exchange bias,<sup>5</sup> and others. Besides their fundamental interest, these phenomena have found industrial applications where they are used to tailor the strength and nature of magnetic interactions. Another known method of changing the magnetic properties of a material is by intercalation of hydrogen.<sup>6,7</sup> The electronic interaction of hydrogen with its host atoms leads to changes of the electronic and magnetic properties of the compound. Consequently, by combining both the effects of the nanoscale and absorption of hydrogen, the modification and control over the magnetic properties can be extended. This can be achieved by selectively changing the electronic properties of one of the constituents in magnetic/nonmagnetic heterostructures. For instance, the switching from antiferromagnetic to ferromagnetic coupling, and vice versa, has been demonstrated for exchange coupled magnetic superlattices.<sup>8-10</sup>

Most studies have concentrated on two dimensional systems, i.e., thin films. Only recently, the study of a three-dimensional (3D) configuration has been reported, in which the magnetic properties of iron particles in a polymer membrane<sup>11</sup> have been determined. The iron nanoparticles in the polymer membrane show superparamagnetic behavior above the blocking temperature following the characteristics of single-domain magnetic nanoparticles. Nevertheless, this experiment was a static approach and therefore a dynamic

study, whereby the magnetic interaction between the nanoparticles is affected as a function of a varying parameter, remains a challenge.

In this work, we dynamically changed the 3D nanoscale magnetism of an iron/vanadium (Fe/V) nanocluster-assembled thin film with hydrogenation. Measurements of the magneto-optical Kerr effect (MOKE) on this material show a dependence of the magnetization on the hydrogen concentration within the film for both increasing and decreasing hydrogen pressure.

## II. SAMPLE PREPARATION, HYDROGEN LOADING, AND SETUP DESCRIPTION

The nanocluster-assembled films were prepared using a dual-target, dual-laser vaporization source. Laser vaporization based cluster sources are currently the most commonly used technique to produce cluster beams, especially for refractory materials.<sup>12</sup> Vaporization of the target material is achieved by the focused light of a high intensity laser. The rapid quenching of the plasma produces clusters.<sup>13,14</sup> A small amount of material is carried by a carrier gas, which also promotes clusterization. The cluster cloud is then expanded into vacuum and forms a cluster beam. The cluster source that was used for this work is described elsewhere in more detail.<sup>15,16</sup> Mass spectra are recorded with a time of flight (ToF) mass spectrometer at various stages of the deposition. Vanadium and iron clusters of 2.8 (0.4) and 2.4 (0.6) nm diameter respectively, were alternately deposited by chopping the laser beams. The nanoclusters were deposited with a base pressure in the vacuum chamber of  $6 \times 10^{-9}$  mbar on a  $4 \times 5$  mm<sup>2</sup> glass substrate. A palladium capping layer was deposited on the cluster-assembled film with an Omicron EFM 3 electron beam evaporator. The palladium capping layer dissociates the H<sub>2</sub> molecules to hydrogen atoms, which are subsequently absorbed allowing atomic hydrogen to enter the Fe/V system.

<sup>a)</sup>Electronic mail: marcel.divece@fys.kuleuven.be.

An x-ray diffraction (XRD) pattern was recorded in a grazing incidence configuration with a PANalytical X'Pert PRO x-ray diffractometer equipped with an ultra fast X'Celerator detector (Cu  $K\alpha$  radiation) as shown in Fig. 1(c). The broad reflections can be indexed with a combination of fcc palladium and bcc iron metal structures. No trace of iron oxide could be detected. Rietveld fitting of the pattern gives cell parameters of 3.896 and 2.869 Å for palladium and iron, respectively, which are very close to literature values (3.8898 and 2.8662 Å). Sizes (diameters) derived according to the Scherrer formula are 9.0 and 5.5 nm for palladium and iron, respectively, indicating aggregation of the iron clusters during deposition. Comparing the size of the iron particles with the ToF mass spectrometer value shows that the aggregates have an average connection length of 2.3 iron nanoclusters. The nanoclusters may have completely merged or are partially connected through a lattice plane.<sup>17</sup> Relative volume fractions of the palladium and iron phases were estimated at approximately 40% and 60%, respectively. This ratio shows that a large part of the iron is not detected due to amorphicity or oxidation. Despite the presence of an amorphous iron oxidic phase, these XRD results clearly show that a significant amount of iron forms a metallic phase. Vanadium was not observed in the XRD pattern, probably due to a combination of a high degree of amorphicity and small size.

Rutherford backscattering spectroscopy (RBS) provides a Fe/V ratio of 2/1. The thickness of the Fe/V cluster-assembled film and the palladium cap layer are 70 and 6.5 nm, respectively. As the nanocluster deposition parameters remained constant during deposition, a concentration gradient is unlikely. RBS revealed that oxygen was able to cross the palladium layer, resulting in the formation of iron and vanadium oxides. Vanadium oxides do not absorb hydrogen around room temperature<sup>18</sup> and will therefore not contribute to hydrogen-induced effects. However, hydrogen is free to move around these oxidized clusters. Although it is not possible to accurately determine the extent of oxidation, from the presence of metallic iron as determined by XRD, the nanocluster assembly is likely not oxidized in the deepest regions of the film, i.e., in the 10 nm closest to the glass substrate. Alternatively, domains of pure metals and oxides could coexist throughout the film. Increasing the palladium cap layer thickness did not prevent this partial oxidation, possibly due to the roughness and high reactivity of the nanocluster film. Some intermixing at the surface of the iron and vanadium nanoclusters cannot be ruled out as was shown for thin film Fe/V multilayers.<sup>19</sup> As a clear influence of hydrogen on the magnetic properties is observed, complete intermixing is not expected. A schematic representation of the nanocluster film is shown in Fig. 1(a).

MOKE experiments were conducted with a laser beam incident on the substrate side of the film where oxidation effects are not expected. The measured magnetic hysteresis loops as shown in Fig. 1(b) confirm this. In agreement with the XRD results, the occurrence of magnetic hysteresis in this material is a clear sign of unoxidized iron since a control measurement with a film which contained mainly iron oxide yields a purely paramagnetic behavior. Furthermore, the

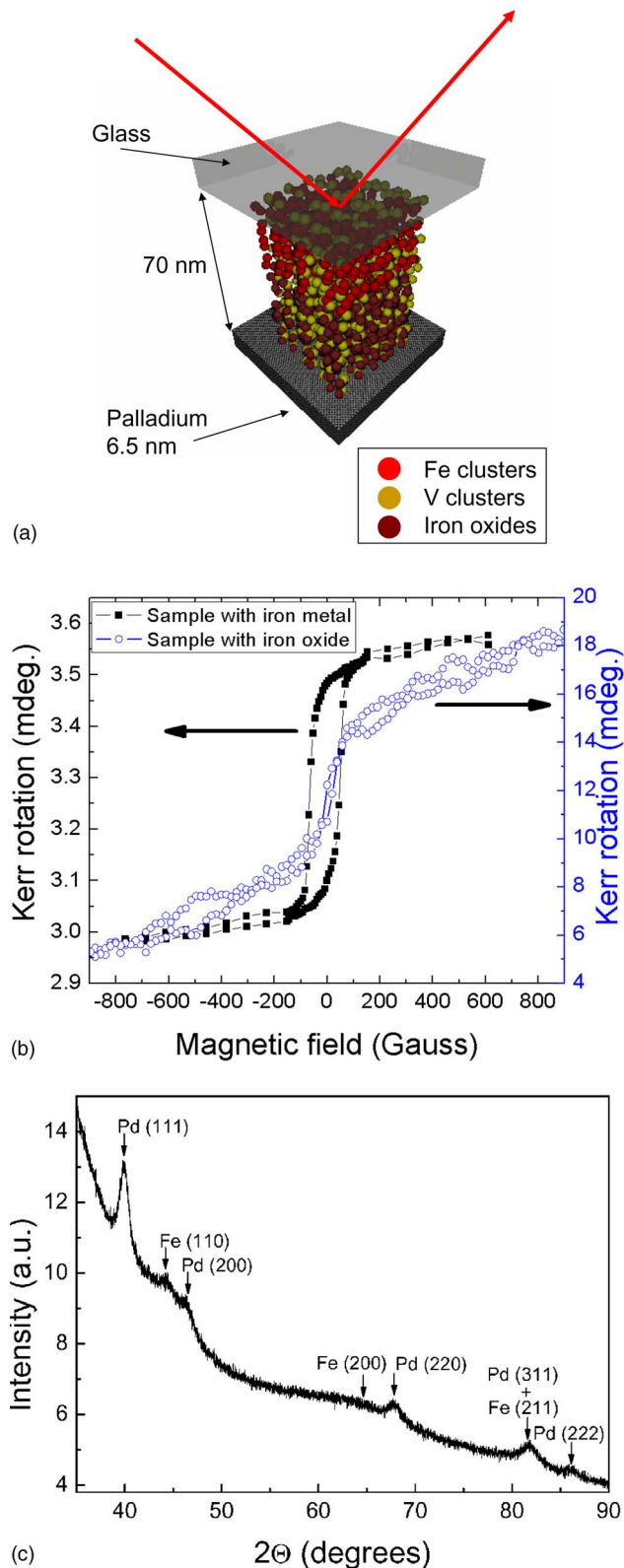


FIG. 1. (Color online) A schematic representation of the likely structure of the nanocluster-assembled thin film (a). The vanadium oxides were omitted for clarity. (b) The Kerr rotation as function of applied magnetic field for the studied sample and for a fully oxidized film, in vacuum. (c) XRD pattern of the as-prepared nanocluster-assembled thin film.

presence of coercivity demonstrates that the iron nanoclusters are aggregated into structures with ferromagnetic rather than superparamagnetic ordering. The superparamagnetic/ferromagnetic transition size lies between 9 and 10 nm in

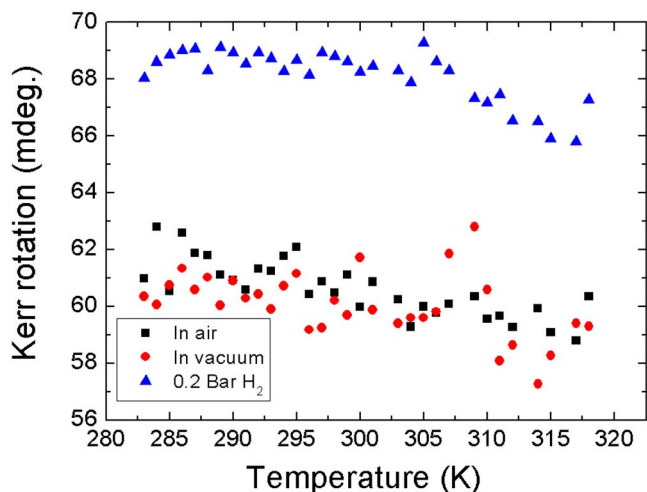


FIG. 2. (Color online) The Kerr rotation as a function of temperature for a sample in ambient air (black squares), in vacuum (red dots) and in 0.2 bar of hydrogen (blue triangles).

diameter as determined by an experimental<sup>20</sup> and a theoretical<sup>21</sup> study. Therefore, most individual clusters behave in a superparamagnetic manner. However, the aggregates of the connected nanoclusters form an entity that is larger than the superparamagnetic limit and should consequently be ferromagnetic. Considering the larger concentration of iron, the iron aggregates may not be completely separated from each other by vanadium nanoclusters. However, the presence of vanadium in between these aggregates allows for a certain amount of magnetic exchange-coupling through the vanadium phase. The MOKE setup consisted of a Melles Griot 56DOL507 continuous wave laser at a wavelength of 830 nm with a maximum power of 35 mW. The light intensity was adjusted by a Melles Griot diode laser driver 06DL03. A polarizer ensured that the incident polarization was along S, i.e., perpendicular to the plane of polarization. After one lens focused the laser beam on the sample, another lens focused the reflected beam on a differential photodetector consisting of a Wollaston prism and two photodiodes, mounted on a precision rotational stage. The signal from the two photodiodes was sent to the channels A and B of a lock-in detector operated in the A-B mode. The lock-in detector was triggered at 1025 Hz by an optical chopper, which was placed in the beam. The precision rotation stage allowed us to calibrate all our measurements by establishing a direct proportionality between the optical rotation in degrees and the measured voltage difference with the lock in. The sample was placed in a hydrogen tight cell, made of optically neutral glass, which allowed the control of the hydrogen pressure with a precision of better than 0.02 bar.

### III. RESULTS AND DISCUSSION

A hysteresis loop similar to the one in Fig. 1(b) has been measured for different temperatures. This provided a Kerr rotation as a function of temperature which is shown in Fig. 2. The Kerr rotation corresponds to the height of the hysteresis loop and is therefore obtained by subtracting the MOKE signals at saturation for positive and negative applied fields of the loop. The Kerr rotation was measured both in vacuum

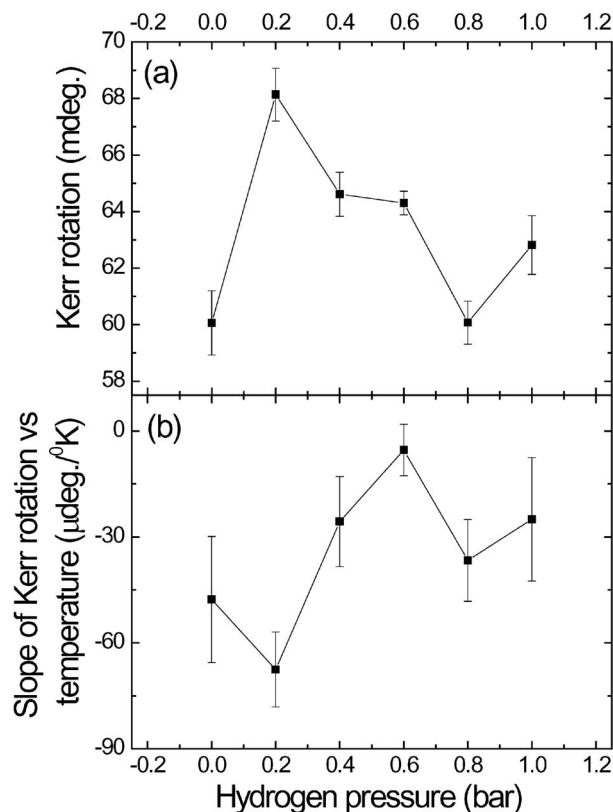


FIG. 3. (a) The Kerr rotation as a function of hydrogen pressure. (b) The slope of the Kerr rotation as a function of temperature, versus hydrogen pressure.

( $\sim 10^{-1}$  mbar) and in ambient air to determine the effect of oxidation which would result in a reduction of the total magnetization and therefore of the MOKE signal. Since no significant difference was observed, this indicates a high stability of the sample against further oxidation. When 0.2 bar of hydrogen was introduced, a clear change in the amplitude of the MOKE signal was observed (blue triangles), as shown in Fig. 2. Furthermore, the decrease of the magnetization as a function of temperature became steeper. The latter phenomenon will be further discussed below. A control measurement on fully oxidized iron and vanadium nanoclusters resulted in the absence of hysteresis and no effects upon hydrogenation were observed as shown in Fig. 1(b).

In Fig. 3, the effect of the hydrogen pressures on the Kerr rotation is presented. It is clear [Fig. 3(a)] that after experiencing a sharp increase when the pressure is raised from 0 to 0.2 bar, the magnitude of the Kerr rotation decreases until the pressure reaches 0.8 bar, while at 1 bar, an increase is again observed. Correspondingly, the slope of the Kerr rotation as a function of temperature initially decreases between 0 and 0.2 bar [see Fig. 3(b)] and subsequently rises for higher pressures. It should be noted that the error bars in Fig. 3(b) do not allow us to resolve the fine features observed for higher pressures in Fig. 3(a). According to the pressure-concentration isotherm of vanadium hydride<sup>22</sup> the pressure range between 0 and 0.2 bar corresponds to about  $\Delta x$  (H/V)=0.75, while further increasing to 1 bar yields an additional change of only  $\Delta x$  (H/V)=0.07. Therefore, the absorption of hydrogen, between 0 and 0.2 bar, strongly influ-

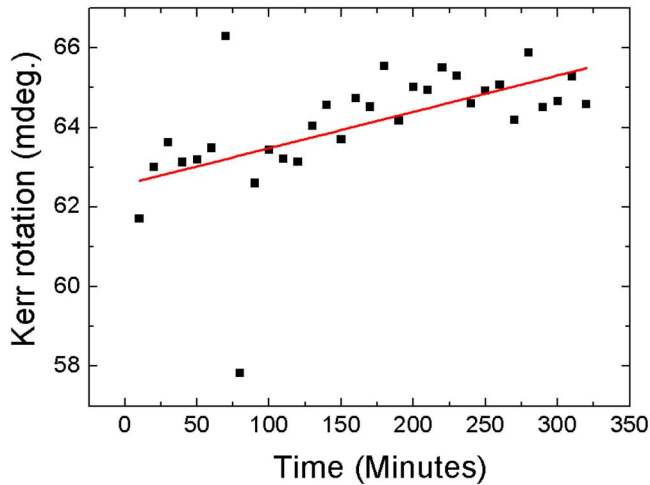


FIG. 4. (Color online) The Kerr rotation as a function of time, starting at a hydrogen pressure of 1 bar, measured at 50 °C.

ences the electronic properties of vanadium, which in turn mediates the exchange coupling between the iron nanocluster aggregates. Consequently, the effect of hydrogen absorption on the magnetic properties explains the change in Kerr rotation.<sup>23</sup>

In order to unambiguously establish the influence of hydrogen on the magnetization, the Kerr rotation was measured as a function of decreasing hydrogen pressure. After the experiment at a hydrogen pressure of 1 bar, the measurement cell was opened to air and the MOKE signal was recorded as a function of time. In order to facilitate the release of hydrogen, the sample temperature was kept at 50 °C. The Kerr rotation increases as function of time as shown in Fig. 4. This can only be attributed to the release of hydrogen from the nanocluster-assembled film.

The distribution of metal and oxidized nanoclusters cannot be established on the sole evidence of magnetic coercivity in Fig. 1(b). The XRD analysis pointed to the formation of iron cluster aggregates with an average size of 2.3 times the size of the gas phase clusters. The iron atoms are two times more numerous than vanadium, which is in agreement with these iron aggregates being surrounded by vanadium nanoclusters. For the discussion of this structure it is necessary to relate the measured dependence of the magnetization on the hydrogen pressure to the fact that, at equilibrium, the hydrogen atoms are confined to the vanadium clusters.<sup>23</sup> The question then arises to what extent the aggregates are connected. If all the iron nanoclusters aggregates were fully connected, then the hydrogen pressure would have no effect on the magnetization. Since we clearly observed a magnetic effect, part of the aggregates must be connected through the vanadium nanoclusters.

As can be seen in Fig. 3(a), the MOKE signal and therefore the magnetization in the sample fluctuates as a function of increasing hydrogen pressure (concentration). This behavior agrees well with an exchange coupling mechanism. In RKKY coupling, the magnetic moment of a metal can be coupled through the conduction band electrons of a neighboring metal without magnetic moment. This particular coupling has an oscillatory dependence on the thickness of the

conducting nonmagnetic spacer. As vanadium expands as a function of hydrogen concentration, this structural change may explain the fluctuations in the Kerr rotation as a function of hydrogen pressure. A more likely mechanism involves a direct change in the electronic properties of vanadium upon hydrogen absorption, as suggested by Hjörvarsson *et al.*<sup>9</sup> on a distortion of the Fermi level.

Additionally, the slope of the magnetic moment versus temperature, which is related to the Curie temperature, exhibits significant variations as shown in Fig. 3(b). These variations accompany the simultaneous changes of the magnetic moment in the film, as measured by the MOKE signal amplitude. Such a relation has been described in a study of exchange coupled Fe/V superlattices.<sup>24</sup> From these arguments, we draw the conclusion that, in this system, magnetic exchange coupling mediated by the vanadium nanoclusters is present between aggregates of iron nanoclusters. Nevertheless, it is to be expected that these aggregated iron nanoclusters are also exchange coupled to a very large aggregate formed by those iron clusters for which the coupling is not affected by hydrogen loading, e.g., because they are physically touching and hence directly coupled without vanadium as a mediator. The presence of such a large aggregate would account for the relatively weak variations of the magnetic moment versus hydrogen pressure. A recent study by Remhof *et al.*<sup>25</sup> shows that the influence of hydrogen on the density of states of the *d*-band changes the magnetic moment of both iron and vanadium at the interface. A future high precision study is necessary to determine the contribution of such an effect in the Fe/V nanocluster assembly.

#### IV. CONCLUSION

In conclusion, the MOKE of iron-vanadium nanocluster-assembled thin films was measured. It was demonstrated that hydrogen has a clear effect on the magnetization of this 3D system for increasing and decreasing hydrogen pressures. Although part of the nanoclusters were oxidized, metallic nanocluster assemblies were present as seen by XRD, which may be distributed throughout the film or likely form a layer close to the substrate allowing the observed effects. The lattice constant and electronic properties of the vanadium mediated nanoclusters are modified by the hydrogen content, which directly influences the exchange coupling between the iron nanostructures. Besides the observed phenomena, the combination of nanoclusters, hydrogen, optics, and magnetism constitutes an experiment of high complexity, which will open a new route for investigating and using 3D nanomagnetic systems. Parameters such as the size, composition, and the ratio between magnetic and nonmagnetic nanoclusters can be varied in future studies.

#### ACKNOWLEDGMENTS

We acknowledge financial support from the Fund for Scientific Research Flanders (FWO), the Belgian Interuniversity Attraction Pole (IAP), Vlaanderen and the K.U.Leuven Research Council (GOA). We wish to thank Rik Stobbe and Frans Hennau for their technical support and Jelle Wouters for helpful discussions.

- <sup>1</sup>S. S. P. Parkin, N. More, and K. P. Roche, *Phys. Rev. Lett.* **64**, 2304 (1990).
- <sup>2</sup>P. Grünberg, R. Schreiber, Y. Pang, M. B. Brodsky, and H. Sowers, *Phys. Rev. Lett.* **57**, 2442 (1986).
- <sup>3</sup>M. N. Baibich, J. M. Broto, A. Fertfert, F. N. Vandau, F. Petroff, P. Eitenne, G. Creutzet, A. Friederich, and J. Chazelas, *Phys. Rev. Lett.* **61**, 2472 (1988).
- <sup>4</sup>A. E. Berkowitz, J. R. Mitchell, M. J. Carey, A. P. Young, S. Zhang, F. E. Spada, F. T. Parker, A. Hutten, and G. Thomas, *Phys. Rev. Lett.* **68**, 3745 (1992).
- <sup>5</sup>W. H. Meiklejohn and C.P. Bean, *Phys. Rev.* **105**, 904 (1957).
- <sup>6</sup>J. Völkl and G. Alefeld, in *Hydrogen in Metals I*, Topics in Applied Physics Vol. 28, edited by G. Alefeld and J. Völkl, (Springer, Berlin, 1978).
- <sup>7</sup>B. Hjörvarsson, C. Chacon, H. Zabel, and V. Leiner, *J. Alloys Compd.* **356–357**, 160 (2003).
- <sup>8</sup>F. Klose, Ch. Rehm, D. Nagengast, H. Maletta, and A. Weidinger, *Phys. Rev. Lett.* **78**, 1150 (1997).
- <sup>9</sup>B. Hjörvarsson, J. A. Dura, P. Isberg, T. Watanabe, T. J. Udovic, G. Andersson, and G. F. Majkrzak, *Phys. Rev. Lett.* **79**, 901 (1997).
- <sup>10</sup>T. Burkert, P. Svedlindh, G. Andersson, and B. Hjörvarsson, *Phys. Rev. B* **66**, 220402 (2002).
- <sup>11</sup>M. Yoon, Y. M. Kim, V. Volkov, H. J. Song, Y. J. Park, S. L. Vasilyak, and I.-W. Park, *J. Magn. Magn. Mater.* **265**, 357 (2003).
- <sup>12</sup>P. Milani and S. Iannotta, *Cluster Beam Synthesis of Nanostructured Materials* (Springer, Berlin, 1999).
- <sup>13</sup>P. Milani and W. A. de Heer, *Rev. Sci. Instrum.* **61**, 1835 (1990).
- <sup>14</sup>S. Maruyama, L. R. Anderson, and R. E. Smalley, *Rev. Sci. Instrum.* **61**, 3686 (1990).
- <sup>15</sup>W. Bouwen, P. Thoen, F. Vanhoutte, S. Bouckaert, F. Despa, H. Weidele, R. E. Silverans, and P. Lievens, *Rev. Sci. Instrum.* **71**, 54 (2000).
- <sup>16</sup>A. N. Dobrynin, D. N. Ievlev, G. Verschoren, J. Swerts, M. J. Van Bael, K. Temst, P. Lievens, E. Piscopiello, G. Van Tendeloo, S. Q. Zhou, and A. Vantomme, *Phys. Rev. B* **73**, 104421 (2006).
- <sup>17</sup>M. Di Vece, D. Grandjean, M. J. Van Bael, C. P. Romero, X. Wang, S. Decoster, A. Vantomme, and P. Lievens, *Phys. Rev. Lett.* **100**, 236105 (2008).
- <sup>18</sup>K. H. Müller, H. Paulus, and G. Kiss, *Appl. Surf. Sci.* **179**, 292 (2001).
- <sup>19</sup>A. Scherz, H. Wende, P. Pouloupoulos, J. Lindner, K. Baberschke, P. Blomquist, R. Wäppling, F. Wilhelm, and N. B. Brookes, *Phys. Rev. B* **64**, 180407 (2001).
- <sup>20</sup>S. Wirth, A. Anane, and S. von Molnár, *Phys. Rev. B* **63**, 012402 (2000).
- <sup>21</sup>W. F. Brown, *Phys. Rev.* **130**, 1677 (1963).
- <sup>22</sup>M. Di Vece, A. Remhof, and J. J. Kelly, *Electrochem. Commun.* **6**, 17 (2004).
- <sup>23</sup>S. Olsson, P. Blomquist, and B. Hjörvarsson, *J. Phys.: Condens. Matter* **13**, 1685 (2001).
- <sup>24</sup>D. Labergerie, K. Westerholt, H. Zabel, and B. Hjörvarsson, *J. Magn. Magn. Mater.* **225**, 373 (2001).
- <sup>25</sup>A. Remhof, G. Nowak, H. Zabel, M. Björck, M. Pärnaste, B. Hjörvarsson, and V. Uzdin, *Europhys. Lett.* **79**, 37003 (2007).